Chemical Engineering Journal 394 (2020) 124881

Contents lists available at ScienceDirect

Chemical Engineering Journal

journal homepage: www.elsevier.com/locate/cej

Kinetic modelling of methanol synthesis over commercial catalysts: A critical assessment

F. Nestler[a,*], A.R. Schütze[a], M. Ouda[a], M.J. Hadrich[a], A. Schaadt[a], S. Bajohr[b], T. Kolb[b]

[a] Fraunhofer-Institute for Solar Energy Systems ISE, Heidenhofstr. 2, 79110 Freiburg, Germany
[b] Engler-Bunte-Institute EBI, Engler-Bunte-Ring 2, Karlsruhe, Germany

HIGHLIGHTS:

- A new kinetic parameter set for a commercial state-of-the-art catalyst is presented.
- The kinetic model presented shows a high accuracy towards the measured data.
- Comparison to literature models proves the plausibility of the model.
- A sensitivity analysis shows the impact of the kinetic model towards reactor design.
- For kinetic measurements in the context of PtM high CO_2 contents must be considered.

GRAPHICAL ABSTRACT

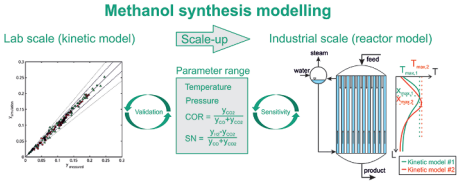

ARTICLE INFO

Keywords:
Methanol synthesis
Kinetic model
CO_2 hydrogenation
Reactor simulation
Power-to-methanol

ABSTRACT

Kinetic modelling of methanol synthesis over commercial catalysts is of high importance for reactor and process design. Literature kinetic models were implemented and systematically discussed against a newly developed kinetic model based on published kinetic data. Deviations in the sensitivities of the kinetic models were explained by means of the experimentally covered parameter range. The simulation results proved that an extrapolation of the working range of the kinetic models can lead towards significant simulation errors especially with regard to pressure, stoichiometric number and CO/CO_2-ratio considerably limiting the applicability of kinetic models frequently applied in scientific literature. Therefore, the validated data range for kinetic models should be considered when detailed reactor simulations are carried out. With regard to Power-to-Methanol processes special attention should be drawn towards the rate limiting effect of water at high CO_2 contents in the syngas. Moreover, it was shown that kinetic models based on data measured over outdated catalysts show significantly lower activity than those derived from state-of-the-art catalysts and should therefore be applied with caution for reactor and process simulations. The plausible behavior of the herein proposed kinetic model was demonstrated by a systematic comparison towards established kinetic approaches within both, an ideal kinetic reactor and an industrial steam cooled tubular reactor. Relative to the state-of-the-art kinetic models it was proven that the herein proposed kinetic model can be applied over the complete industrially relevant working range for methanol synthesis.

* Corresponding author.
E-mail address: florian.nestler@ise.fraunhofer.de (F. Nestler).

https://doi.org/10.1016/j.cej.2020.124881
Received 9 December 2019; Received in revised form 13 March 2020; Accepted 23 March 2020
Available online 25 March 2020
1385-8947/

Nomenclature

A_R	cross sectional area of the reactor (m^2)
$c_{p,gas}$	molar heat capacity of gas mixture (kJ mol^{-1} K^{-1})
COR	carbon oxide ratio (–)
d_{int}	inner diameter of the reaction tube (m)
d_{ext}	external diameter of the reaction tube (m)
d_P	particle diameter (m)
EQ_1	equilibrium term for CO_2 hydrogenation (–)
EQ_2	equilibrium term for reverse water-gas-shift reaction (–)
f_j	fugacity of component j (Pa)
$GHSV$	gas hourly space velocity (h^{-1})
H_{cat}	axial length of the catalyst bed (m)
k_1	reaction rate constant for CO_2 hydrogenation based on weight of the catalyst (mol kg^{-1} s^{-1} Pa^{-1})
k_2	reaction rate constant for reverse water-gas-shift reaction based on weight of the catalyst (mol kg^{-1} s^{-1} $Pa^{-0.5}$)
K_1	adsorption constant for CO (Pa^{-1})
$K_{1,B}$	merged parameter of the Bussche model (–)
K_2	adsorption constant for CO_2 (Pa^{-1})
$K_{2,B}$	adsorption constant for H_2 of the Bussche model ($Pa^{-0.5}$)
K_3	adsorption constant for H_2O and H_2 ($Pa^{-0.5}$)
$K_{3,B}$	adsorption constant for H_2O of the Bussche model (Pa^{-1})
$K_{eq,1}$	equilibrium constant for CO_2 hydrogenation (Pa^{-2})
$K_{eq,2}$	equilibrium constant for reverse water–gas-shift reaction (–)
N_{points}	number of experimental points (–)
N_{tubes}	number of tubes (–)
$\dot{n}_j$	molar flow of component j (mol s^{-1})
	total molar flow (mol s^{-1})
p	synthesis pressure (bar)
r_i	reaction rate of reaction i based on weight of the catalyst (mol s^{-1} kg^{-1})
R	universal gas constant (J mol^{-1} K^{-1})
$RMSE_i$	root mean square error of molar fractions for component i (–)
SN	stoichiometric number (–)
SUM	sum of RMSE values for optimization (–)
T	temperature inside reactor (K)
T_{cool}	temperature of steam cooling (K)
T_{in}	inlet temperature of reactor (K)
T_{max}	temperature of hot spot (K)
U_{tot}	overall heat transfer coefficient (W m^{-2} K^{-1})
x	axial distance in the reactor (m)
x_{max}	axial location of the hot spot (m)
y_j	molar fraction of component j (–)

Greek letters

ΔH_R^0	enthalpy of reaction at standard conditions (J mol^{-1})
$\Delta H_{R,i}$	enthalpy of reaction i at reaction conditions (J mol^{-1})
ρ_{bulk}	bulk density of the catalyst (kg m^{-3})
ν_j	stoichiometric coefficient of component j (–)

1. Introduction

With an annual production of almost 90 million metric tons methanol is one of the most important commodity chemicals in the world [1]. After BASF invented the first commercial process for thermochemical methanol production in 1923, the synthesis process was continuously developed further by the scientific community and industry [2]. In 1966 ICI patented the first commercially applied low pressure synthesis process enabling pressures below 150 bar and temperatures under 300 °C by applying a Cu-Zn based catalyst [3,4]. Until today, this catalytic system is mainly applied in industrial processes, however, catalyst manufacturers and scientists are frequently reporting on enhancements by means of activity and catalyst lifetime [4].

Recently, methanol synthesis is facing a lot of research activity due to so-called Power-to-Methanol (PtM) processes, where methanol can be produced from industrial CO and CO_2 (e.g. captured from flue gas, steel industry, biogas or air) and H_2 based on electrolysis of water [3,5–7]. The gas compositions and operating conditions in PtM processes differ significantly from commercial processes based on natural gas reforming, heavy oil fractions or coal gasification [8]. Vivid research is performed aiming to invent catalysts with enhanced activity and stability under these conditions [9,10]. Besides that researchers are actively enhancing the process conditions and layouts in order to improve economics and decrease the ecological impact of PtM processes [11–13].

Despite the high research activity on the methanol synthesis in the past century, the exact surface mechanism is not completely known today [9]. However, hypotheses have been made by many researchers for the formulation of kinetic models [2]. While many of these models are based on self-prepared catalysts with the drawback of difficult reproducibility [7,14–17], some researchers used commercial catalysts for their work [18–22]. As temperature in industrial methanol synthesis reactors is limited due to thermal sintering, an adequate simulative description of the temperature profile inside the reactor is of vital importance [2,23]. From a practical approach, application of kinetic models measured over commercial catalysts appears a promising option. Meyer et al. performed a comparison of the two established kinetic models by Graaf [22] and Bussche [18] within an industrial process simulation [24]. However, a systematic comparison of these established kinetic models towards recently developed models based on up-to-date catalysts is not provided in scientific literature [19,20]. Moreover, in the field of methanol synthesis no studies are available explaining differences in the behavior of the kinetic models by means of their respective experimental validation parameter range. Therefore, this work aims to show the differences between four kinetic models based on commercial catalysts including one newly developed kinetic model derived from previously published experimental data. A comprehensive sensitivity study is performed over a wide working range of industrial and PtM methanol synthesis conditions in order to show both the importance of the experimental data basis and the catalyst considered on the quality of the reactor simulation. Discrepancies in the kinetic behavior are traced back towards the experimental validation data basis. Moreover, differences between the herein published kinetic model and two important literature standards are elaborated to show the relevance of updated kinetic models for the scientific community.

2. Material and methods

Besides the comparison of theoretical kinetic model parameters, i.e. adsorption constants and reaction rates, this paper will also discuss different kinetic models in the context of their application within an industrial methanol synthesis reactor. Therefore, the key features of state-of-the-art methanol synthesis will be shortly introduced. After that, the considered kinetic models are described and the fitting procedure for experimental data will be explained briefly before the parameters for the sensitivity study are presented.

2.1. Methanol synthesis

Industrial methanol synthesis is performed in a thermochemical loop process from synthesis gas (syngas), i.e. a mixture of H_2, CO and CO_2. Syngas is commercially supplied by natural gas reforming and coal

gasification [25] or in case of a PtM process from industrial carbon oxide containing off-gas and hydrogen from water electrolysis [26]. The syngas is mixed upstream of the methanol reactor with unconverted recycle gas to obtain the reactor feed gas. Inside the reactor the following equilibrium reactions occur over a $Cu/Zn/Al_2O_3$ catalyst [27]:

$$CO_2 + 3H_2 \rightleftarrows CH_3OH + H_2O \ \Delta H_R^0 = -50\ kJ{\bullet}mol^{-1} \quad (1)$$

$$CO + H_2O \rightleftarrows CO_2 + H_2 \ \Delta H_R^0 = -41\ kJ{\bullet}mol^{-1} \quad (2)$$

$$CO + 2H_2 \rightleftarrows CH_3OH \ \Delta H_R^0 = -91\ kJ{\bullet}mol^{-1} \quad (3)$$

Within this reaction network methanol synthesis was proven to mainly appear via CO_2 hydrogenation [28–30]. All three reactions, CO_2 hydrogenation (Eq. (1)), water-gas-shift reaction (WGS, Eq. (2)) and CO hydrogenation (Eq. (3)) are exothermic. WGS is mainly depending on concentration of the reactants and temperature. Increased CO_2 partial pressures in the syngas can therefore lead towards the reverse WGS (rWGS). The hydrogenation reactions reduce the number of moles. Therefore, according to Le Chatelier's principle high equilibrium conversions can be achieved at low temperatures and high pressures [31]. However, temperatures above 200 °C are necessary in order to obtain considerable reaction rates on state-of-the-art catalysts [32]. On the other hand temperatures exceeding 300 °C are known to lead towards fast catalyst deactivation [23,33]. Therefore, the reaction is carried out in a narrow temperature operation window between 220 °C and 280 °C. Typical synthesis pressures for industrial applications range between 50 bar and 100 bar [32]. The composition of the synthesis gas can be determined by the following key parameters:

$$SN = \frac{y_{H_2} - y_{CO_2}}{y_{CO} + y_{CO_2}} \quad (4)$$

$$COR = \frac{y_{CO_2}}{y_{CO} + y_{CO_2}} \quad (5)$$

The stoichiometric number (SN) defines the ratio between H_2 and carbon oxides [34]. $SN = 2$ would be a stoichiometric mixture, however, in industrial processes an excess of H_2 is provided in the syngas to avoid side product formation [32]. The carbon oxide ratio (COR) defines the ratio between CO_2 and CO in the syngas [8]. In conventional processes COR is usually held below 0.6 [8]. Increased CO_2 contents are known to decrease the reaction kinetics, equilibrium conversion and lead towards faster catalyst deactivation due to enhanced sintering processes but have the advantage of a lower selectivity towards carbonaceous side products [33,35–39]. As PtM processes mainly utilize CO_2 based syngas, a COR close to unity must be considered for these technologies [8].

2.2. Reactor modelling

Within this publication the isothermal tube bundle reactor as described in literature is utilized to discuss the differences between the different kinetic models considered within this study [40–43]. One dimensional modelling of the synthesis reactor is based on the following set of balance equations:

Material balance:

$$\frac{d\dot{n}_j}{dx} = \rho_{bulk}{\bullet}A_R{\bullet}\sum \upsilon_j{\bullet}r_i \quad (6)$$

Energy balance:

$$\frac{dT}{dx} = \frac{\sum \Delta H_{R,i}{\bullet}r_i{\bullet}A_R{\bullet}\rho_{bulk}}{c_{p,gas}{\bullet}\dot{n}_{tot}} + \frac{\pi{\bullet}d_{int}{\bullet}U_{tot}{\bullet}(T_{cool} - T)}{c_{p,gas}{\bullet}\dot{n}_{tot}} \quad (7)$$

Equations for the calculation of the overall heat transfer coefficient U_{tot} are based on the α_w model described in VDI heat atlas [44]. Physical properties are calculated according to NIST database. Design parameters for the synthesis reactor set-up are given in Table 1 [40–43]. As this work aims to compare different kinetic models isolated from the influence of diffusion limitations, these are not accounted for within this work. According to the Ergun equation a maximum pressure loss of 2.2 bar along the fixed bed was calculated for the industrial reactor simulation cases considered within this study [2,24,44]. As this did not significantly affect the simulation results, pressure loss was not further considered within this study.

The reactor model was verified by comparison with other publications performing similar simulations with the proposed kinetic models [18,24].

2.3. Kinetic modelling of methanol synthesis

In the context of this publication, a kinetic model is defined by the combination of the kinetic rate equations and the respective kinetic parameter set. The kinetic model defined by Graaf in 1988 is mechanistically based on the stepwise hydration of adsorbed CO and CO_2 on two active sites [22]. The parameter set for the model was updated by the authors in 1990 [45]. In their experimental studies the authors utilized a spinning basket reactor filled with a commercial MK-101 catalyst produced by Haldor Topsøe. Even though their kinetic model was published almost 30 years ago, it is still applied within recent simulation studies [24,46–48]. The mechanism, kinetic rate equations and parameter set are provided in Appendix A (parameter set see Table 6).

In 1996 Bussche and Froment [18] published a kinetic model, which became another important literature standard through the last decades [11,12,24,49,50]. The authors proposed a mechanism via the carbonate species on one active site. In their kinetic measurements a fixed bed reactor filled with the ICI 51-2 catalyst was used. Other than in the model of Graaf, no direct CO hydrogenation reaction was considered. By doing so, the authors accounted for current research results stating that methanol is mainly produced by CO_2 hydrogenation. Further details of the kinetic model by Bussche et al. are given in Appendix B (parameter set see Table 7).

In 2011, Graaf's kinetic model was updated by Henkel during his doctoral studies performing a comprehensive kinetic study utilizing a commercial catalyst by Südchemie (today Clariant) [19]. Henkel used two different experimental set-ups, i.e. a Berty reactor and a micro fixed bed reactor. Due to results published by the scientific community and the quality of his parameter fitting, CO hydrogenation was not considered within his final kinetic model. The mechanism for rWGS and CO_2 hydrogenation was overtaken from Graaf's kinetic model. Henkel ascribed the kinetic rate equation in the following form:

$$r_{CO_2} = \frac{k_1{\bullet}K_2{\bullet}f_{CO_2}{\bullet}f_{H_2}^{1.5}{\bullet}EQ_1}{(1 + K_1{\bullet}f_{CO} + K_2{\bullet}f_{CO_2}){\bullet}(f_{H_2}^{0.5} + K_3{\bullet}f_{H_2O})} \quad (8)$$

$$r_{rWGS} = \frac{k_2{\bullet}K_2{\bullet}f_{CO_2}{\bullet}f_{H_2}{\bullet}EQ_2}{(1 + K_1{\bullet}f_{CO} + K_2{\bullet}f_{CO_2}){\bullet}(f_{H_2}^{0.5} + K_3{\bullet}f_{H_2O})} \quad (9)$$

As Henkel could not obtain one kinetic parameter set for the two experimental setups used within his studies he proposed the two parameter sets listed in Table 2.

Table 1
Reactor design parameters based on literature [40–43].

Parameter	Unit	Value
d_{int}	m	0.038
d_{ext}	m	0.042
H_{cat}	m	7.022
N_{tubes}	–	1
d_P	m	0.005
T_{in}	°C	230
T_{cool}	°C	252

Table 2
Kinetic parameters fitted by Henkel for the Berty reactor and the micro fixed bed reactor [19].

	Unit	Berty	Micro fixed bed
k_1	$mol \cdot kg^{-1} \cdot s^{-1} \cdot Pa^{-1}$	$4.629 \cdot 10^{-4} \cdot \exp\frac{-47,472}{R \cdot T}$	$3.172 \cdot 10^{-4} \cdot \exp\frac{-45,893}{R \cdot T}$
k_2	$mol \cdot kg^{-1} \cdot s^{-1} \cdot Pa^{-0.5}$	$12.975 \cdot \exp\frac{-60,609}{R \cdot T}$	$2.021 \cdot 10^{6} \cdot \exp\frac{-112,322}{R \cdot T}$
K_1	Pa^{-1}	$2.743 \cdot 10^{-17} \cdot \exp\frac{108,082}{R \cdot T}$	$2.420 \cdot 10^{-14} \cdot \exp\frac{81,976}{R \cdot T}$
K_2	Pa^{-1}	$1.935 \cdot 10^{-4}$	$1.000 \cdot 10^{-4}$
K_3	$Pa^{-0.5}$	$5.797 \cdot 10^{-14} \cdot \exp\frac{112,322}{R \cdot T}$	$1.040 \cdot 10^{-8} \cdot \exp\frac{61,856}{R \cdot T}$

The equilibrium terms EQ_1 and EQ_2 are calculated from the equilibrium constants $K_{eq,1}$ and $K_{eq,2}$ with regard to the expression published by Graaf et al. in 2016 [51].

$$EQ_1 = 1 - \frac{f_{MeOH} \cdot f_{H_2O}}{f_{CO_2} \cdot f_{H_2}^3 \cdot K_{eq,1}} \tag{10}$$

$$EQ_2 = 1 - \frac{f_{CO} \cdot f_{H_2O}}{f_{CO_2} \cdot f_{H_2} \cdot K_{eq,2}} \tag{11}$$

The fugacities for the components are calculated according to the equation-of-state published by Soave-Redlich-Kwong (SRK) [52].

Park et al. used a commercial Clariant state-of-the-art catalyst within their kinetic fixed bed studies in 2014 [20]. The kinetic model they proposed was based on the original reaction mechanism provided by Graaf [22] coupled with an additional DME kinetic model published by Chadwick et al. [53]. However, their kinetic rate equations still did account for CO hydrogenation and included the DME kinetics originally measured over another catalyst. Moreover, the parameter set resulting from their parameter fitting was not completely provided within their publication. Therefore, the kinetic model published by Park et al. is not explicitly treated within this study. Nonetheless, as the authors published a complete experimental data set of their experiments, this data will be used for validation and parameter regression within this study.

All kinetic models considered within this study are based on experimental data measured over commercial catalysts. However, the validated parameter ranges in terms of temperature (Fig. 1 A), pressure (Fig. 1 B), SN (Fig. 1 C) and COR (Fig. 1 D) significantly differ for the different data sets. All kinetic models cover the temperature ranges relevant for industrial methanol synthesis. In terms of synthesis pressure, Graaf and Bussche only validated their kinetic model for pressures up to 50 bar, whereas Henkel and Park considered higher synthesis pressures up to 75 bar and 90 bar, respectively. As industrial methanol synthesis is usually carried out at pressures exceeding 50 bar, this is a major drawback of the two literature standard models proposed by Bussche and Graaf [54]. An important factor influencing the kinetic performance is the stoichiometric number applied in the kinetic studies. Unfortunately, for this key parameter no data were provided by Bussche et al. [18]. Therefore it is left unclear, for which SN-range their kinetic model was derived. While Graaf and Henkel measured both, sub- and over-stoichiometric conditions, Park et al. did not investigate the reaction kinetics at H_2 shortage for their model (i.e. SN < 2.0). COR greatly influences the kinetics of methanol synthesis as water produced by CO_2 hydrogenation considerably limits the reaction kinetics [55]. This effect is enhanced with increasing COR [56]. Within the context of PtM technologies it therefore needs to be mentioned that Henkel's kinetic model probably does not account for these limitations as he performed measurements only until COR = 0.57 (Berty) and COR = 0.93 (fixed bed).

In order to obtain a kinetic model applicable towards a wide working range of conventional and renewable feedstock based methanol synthesis, a kinetic model considering the aforementioned aspects based on a state-of-the-art catalyst should be made available. Application of the kinetic rate equations published by Henkel (i.e. Eq. (1) and (2)) refitted with the experimental data published by Park et al. was presumed to lead towards this desired kinetic model. The model parameters will be compared to those elaborated by Henkel. The macroscopic effect of the kinetic model presented within this study in comparison to state-of-the-art models will be discussed within a comprehensive sensitivity study utilizing the 1D–model of an industrial methanol synthesis reactor presented previously in section 2.1.

2.4. Parameter fitting

For the re-fitting of the measured data set provided in the publication by Park et al. [20], a parameter screening and pre-selection of the data was performed. As the proposed mechanism by Henkel does not consider the CO hydrogenation, measured values with COR = 0.00 were not considered within this study. Four experimental points were therefore excluded from the data set. The remaining 114 measured values were used for the parameter fitting within this study. Based on C, H, O balances, the mole fractions at the reactor exit were determined from the CO and CO_2 conversion given in the original publication. This calculation procedure was performed in order to decrease the sensitivity of the parameter fitting towards measurement errors at low concentrations. Before this procedure was applied, high conversion rates at low total concentrations did greatly affect the resulting model parameters especially when measurements at low COR were included to the fitting. Therefore, it is concluded that the measurement campaign by Park et al. could be affected by measurement errors especially at low concentrations of CO_2. This statement, however, needs to be validated by additional experimental data.

For the fitting procedure the data were imported into a MATLAB® reactor model of the kinetic reactor as documented by Park et al. [20]. The simulated output values were then compared against the measured data by means of the root mean square error (RMSE). RMSE was calculated for the molar fractions of CO and CO_2 as follows:

$$SUM = RMSE_{CO_2} + RMSE_{CO} \tag{12}$$

$$RMSE_{CO_2} = \sqrt{\frac{\sum (y_{CO_2,calc} - y_{CO_2,exp})^2}{N_{points}}} \tag{13}$$

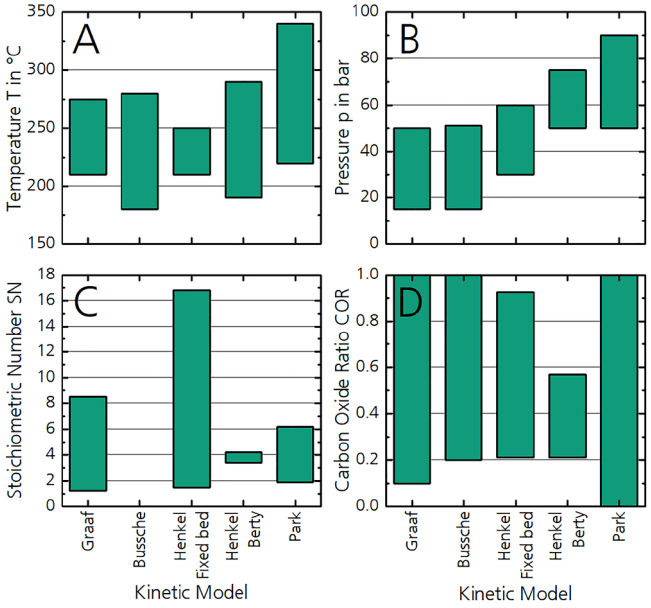

Fig. 1. Range of experimental validation conditions applied by Graaf [22], Bussche [18], Henkel [19] and Park [20] with regard to temperature (A), synthesis pressure (B), stoichiometric number (C) and carbon oxide ratio (D).

$$RMSE_{CO} = \sqrt{\frac{\sum (y_{CO,calc} - y_{CO,exp})^2}{N_{points}}} \quad (14)$$

The sum of the RMSE values for CO and CO_2 was minimized by adaption of the ten model parameters with the starting values taken from Henkel's original parameter set (see Table 2). For minimization, the multidimensional unconstrained non-linear Nelder-Mead algorithm implemented within the fminsearch-method by MATLAB® was applied [57].

2.5. Sensitivity study

In order to evaluate the scientific contribution and validity of the kinetic model proposed within this work, a sensitivity study varying reactor parameters over a wide range was conducted. The proposed kinetic model is directly compared with the established kinetic models by Graaf and Bussche as well as Henkel. The parameter range of the sensitivity analysis is provided in Table 3; A wide range of COR and SN was considered for three pressure levels. Data analysis was performed with focus on the hot spot temperature and position, as the temperature profile is one key feature for industrial reactor design and greatly affected by the reaction kinetics [24,43,58–61]. Dimensions of the reactor were applied with regard to Table 1. All combinations of COR and SN were varied ending up at a parameter set with 20 simulation runs for each kinetic model and pressure level.

3. Results and discussion

3.1. Kinetic model proposed

In Fig. 2 the final fitting result is presented in a parity plot comparing the measured and simulated molar fractions of CO and CO_2 at the exit of the kinetic reactor. The plot illustrates, that most values lie within the 20% trust region. RMSE values of 0.042 and 0.084 remain after the fitting for the CO and CO_2 molar fractions, respectively. Generally, the model describes the whole range of the measured data set in the acceptable range. Importantly, the kinetic model proposed within this study does not constitute a final kinetic expression, but rather a working base which can be complemented during future studies. Further measured data will be necessary in order to validate the model on a wider experimental base.

The kinetic parameters obtained from the fitting procedure are given in Table 4. In agreement with literature findings the reaction rate constants for CO_2 hydrogenation (k_1) and rWGS (k_2) increase with increasing temperature [18,22,62].

While the adsorptions constants for CO (K_1) as well as H_2O and H_2 (K_3) decrease with increasing temperature, the adsorption constant for CO_2 (K_2) does not show any temperature dependence. This finding is in line with the parameter estimation by Henkel who also did not determine a temperature dependence of this constant [19].

In Table 5 the remaining RMSE values for the measured data and the kinetic models by Graaf, Bussche and Henkel as well as the proposed kinetic model are listed. It can be concluded that the model by Graaf shows the highest deviation from the measured data and is therefore not appropriate for the description of the kinetic data considered in this study. A better fitting result could be achieved with the models by Bussche and Henkel. However, due to the fitting procedure applied within this work, it was possible to decrease the deviation by 19.2% for CO and 2.4% for CO_2 with regard to the closest literature model, i.e. Henkel Berty (2011). The remaining error could be due to inaccuracies in the measured data set or an insufficient mechanistic assumption within the proposed model equation. Further investigations will be necessary in order to get a more reliable kinetic description.

The parameters determined by Henkel (see Table 2) are compared towards the parameter set proposed within this study in Fig. 3 by means of Arrhenius diagrams between 200 °C and 320 °C. The figure shows differences in the temperature dependence of both, adsorption and reaction constants between the proposed model and Henkel's model. For the proposed model k_1 (CO_2 hydrogenation) and k_2 (rWGS) are higher in comparison to those by Henkel over the whole temperature range considered.

K_1, i.e. the adsorption constant for CO, of the proposed kinetic model is below the parameter range determined by Henkel for both, Berty and fixed bed reactor. K_2 representing the adsorption constant of CO_2 was computed at a lower value in comparison to Henkel. K_3 representing the adsorption constant of water and H_2 has due to the structure of Eq. (8) and (9) the highest sensitivity on the reaction rate for CO_2-rich syngas. At temperatures exceeding 300 °C the values for K_3 are in a comparable range to those obtained by Henkel with the fixed bed reactor. At lower temperatures, however, increased values for K_3 were determined leading to decreased reaction kinetics at high partial pressures of water in the reacting gas mixture in comparison to the model by Henkel. As high partial pressures of water are known to occur with increasing COR, this finding may be explained by the experimental range covered by Henkel and Park. While Park et al. considered COR up to unity, Henkel did not perform experiments at COR exceeding 0.9 within his study. Hence, Henkel could not account for the rate limiting effect of high water contents in the reaction product within his study (see Fig. 1).

3.2. Comparison of the reaction rates

In order to show the influence of product formation on the reaction rates, the proposed kinetic model is discussed in comparison to the kinetic models by Graaf, Bussche and Henkel for different levels of reaction products formed (see Fig. 4). Temperature dependent reaction rates were calculated for CO_2 hydrogenation at 50 bar with a feed composition of COR = 1.0 and SN = 2.0. Three cases were considered, (A) without product, (B) with 0.5 mol-% of methanol and 1.7 mol-% of water and (C) 1.6 mol-% of methanol and 4.5 mol-% of water. Increased product contents correspond to typical gas compositions in an industrial reactor at this feed composition. Fig. 4 (A) shows that the reaction rate of CO_2 hydrogenation without products in the gas mixture calculated by Bussche's kinetic model is more than one order of magnitude higher than those calculated with the other kinetic models. The reaction rates calculated with Henkel's parameter set show a similar trend as the proposed model, however, at slightly lower level. The lowest reaction rates were calculated using Graaf's kinetic model.

At increased product formation (i.e. 1.7 mol-% water and 0.5 mol-% methanol, (Fig. 4 (B)) the reaction rates calculated by Bussche drop significantly. While Bussche's kinetic model shows a maximum reaction rate at approx. 300 °C the reaction rate of the proposed model increases with rising temperature comparable to the models by Henkel and Graaf. At temperatures below 270 °C the reaction rate of the proposed model falls below that of Henkel's models.

The limiting effect of the products formed towards the reaction rates for the model by Bussche and the proposed model is enhanced when more water and methanol are formed within the reactor (Fig. 4C). Below 300 °C the reaction rates calculated with the models by Henkel and Graaf are slightly decreasing, however, the limiting effect of water is not as strongly developed as in the model published by Bussche and the model proposed within this publication. At 1.6 mol-% of methanol

Table 3
Parameter set varied within the sensitivity study of this publication.

Parameter	Unit	Values
p	bar	50; 65; 80
COR	–	0.25; 0.5; 0.75; 1.0
SN	–	1.5; 2.0; 2.5; 3.0; 3.5

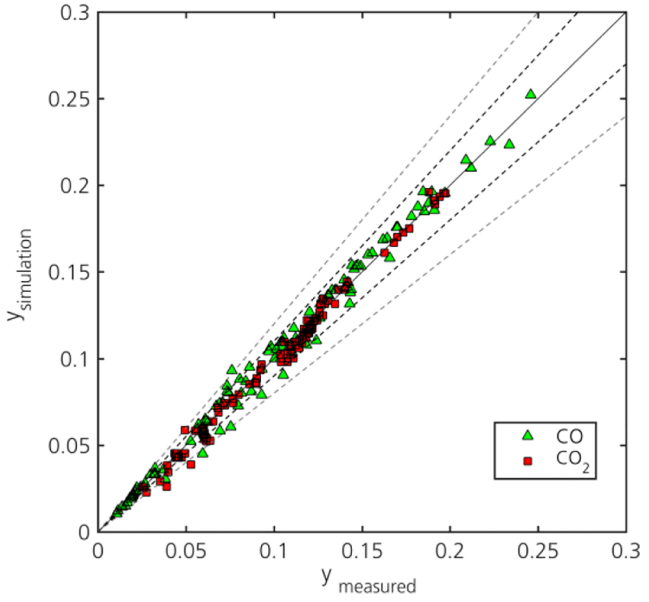

Fig. 2. Parity plot of the kinetic model fitted based on the measured data obtained by Park et al. [20] including the error lines for 0% (solid, black), 10% (dashed, black) and 20% (dashed, grey).

Table 4
Kinetic model parameters for the proposed within this publication.

	Unit	Proposed kinetic parameters
k_1	$mol \cdot kg^{-1} \cdot s^{-1} \cdot Pa^{-1}$	$5.411 \cdot 10^{-4} \cdot \exp\frac{-45,458}{R \cdot T}$
k_2	$mol \cdot kg^{-1} \cdot s^{-1} \cdot Pa^{-0.5}$	$24.701 \cdot \exp\frac{-54,970}{R \cdot T}$
K_1	Pa^{-1}	$3.321 \cdot 10^{-18} \cdot \exp\frac{109,959}{R \cdot T}$
K_2	Pa^{-1}	$8.262 \cdot 10^{-6}$
K_3	$Pa^{-0.5}$	$6.430 \cdot 10^{-14} \cdot \exp\frac{119,570}{R \cdot T}$

Table 5
Comparison of the RMSE for the measured molar fractions by Park and the modelled molar fraction utilizing the kinetic models by Graaf , Bussche, Henkel and the proposed model.

Kinetic model	$RMSE_{CO}$	$RMSE_{CO2}$
Graaf	0.169	0.088
Bussche	0.065	0.085
Henkel, Berty	0.052	0.085
Henkel, fixed bed	0.055	0.085
Proposed	0.042	0.083

and 4.5 mol-% of H_2O the equilibrium limitation of the reaction can be determined at approx. 325 °C.

Concerning the influence of COR on the reaction rates, in scientific literature a maximum conversion to methanol was reported for a reaction mixture with approx. 2 mol-% of CO_2 [16,29,55,63–70]. In Fig. 5 the carbon conversion of an ideally cooled isothermal reactor was calculated at a pressure of 50 bar and a constant temperature of 250 °C for the kinetic models considered. COR was varied from 0.001 towards 1.0 with SN fixed towards 2.0. In order to compare the carbon conversion within the kinetic regime, a GHSV of 20.000 h^{-1} was selected.

The simulation results show a maximum carbon conversion at low COR for all kinetic models, however with Graaf indicating the lowest sensitivity towards COR, i.e. 12.3% and 7.5% for COR = 0.001 and COR = 1.0, respectively. In comparison to the other kinetic models the activity of Graaf's kinetic model is at the lowest level. This finding is in good agreement with those by other researchers stating a low activity of

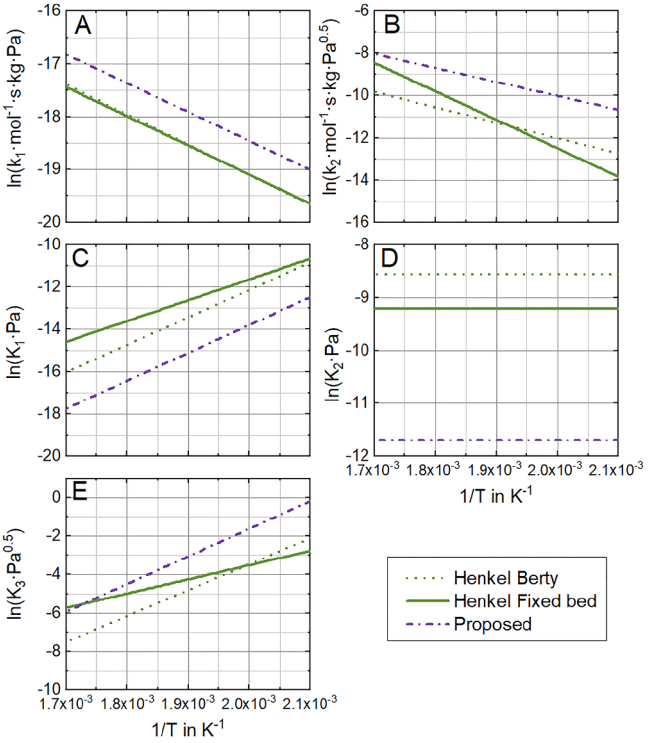

Fig. 3. Arrhenius plot of the kinetic constants k_1 (A), k_2 (B), K_1 (C), K_2 (D), and K_3 (E) for the proposed model in comparison to those calculated with the model by Henkel [19] between 200 °C and 320 °C.

Graaf's kinetic model [59]. Bussche's model indicates the highest influence of COR towards carbon conversion with a maximum of 47.4% achieved at COR = 0.16 (i.e. 5.1 mol-% of CO_2). This maximum is, however, not based on kinetic measurements as the authors did not consider values at COR < 0.2. At COR = 1.0 (i.e. 25.0 mol-% of CO_2) carbon conversion calculated with Bussche's model decreases towards the values obtained by Graaf.

The kinetic model proposed by Henkel shows a maximum carbon conversion of 29.1% at COR = 0.11 (i.e. 3.4 mol-% CO_2) with the Berty parameter set and 23.8% at COR = 0.17 (i.e. 5.2 mol-% CO_2) with the parameter set derived from the fixed bed experiments, respectively. While the simulations with the Henkel kinetics show lower activities than the Bussche model for low COR, higher conversions are obtained at COR exceeding 0.80 and 0.84 for the Berty and the fixed bed parameters, respectively. These high conversions predicted by Henkel's kinetics again show the necessity to provide an appropriate data basis especially for the rate limiting effect of water at high COR.

The kinetic model proposed shows a maximum carbon conversion of 30.5% at COR = 0.18 (i.e. 5.5 mol-% of CO_2) in the reactor feed and is therefore within the range of the models proposed by Henkel (fixed bed) and Bussche with regard to the gas composition. The considerably higher carbon conversion of Bussche's kinetic model in comparison to that of Henkel and the proposed model could be due to weak validation data of the kinetic data set by Bussche at low COR and SN = 2.0. Slightly increased carbon conversion is obtained at COR = 1.0 by the proposed model in comparison to Bussche and Graaf. With 8.4% this value is, however, well below the prediction made by the Henkel's kinetic models at 12.7% and 11.7% for Berty and fixed bed parameters, respectively.

3.3. Comparison of reactor simulations

1D-temperature and product concentration profiles simulated for a steam cooled tubular reactor utilizing the proposed kinetic model and Bussche's model are provided in Fig. 6. As inlet parameters for the syngas COR = 0.75 and SN = 2.0 at a pressure of 65 bar were selected.

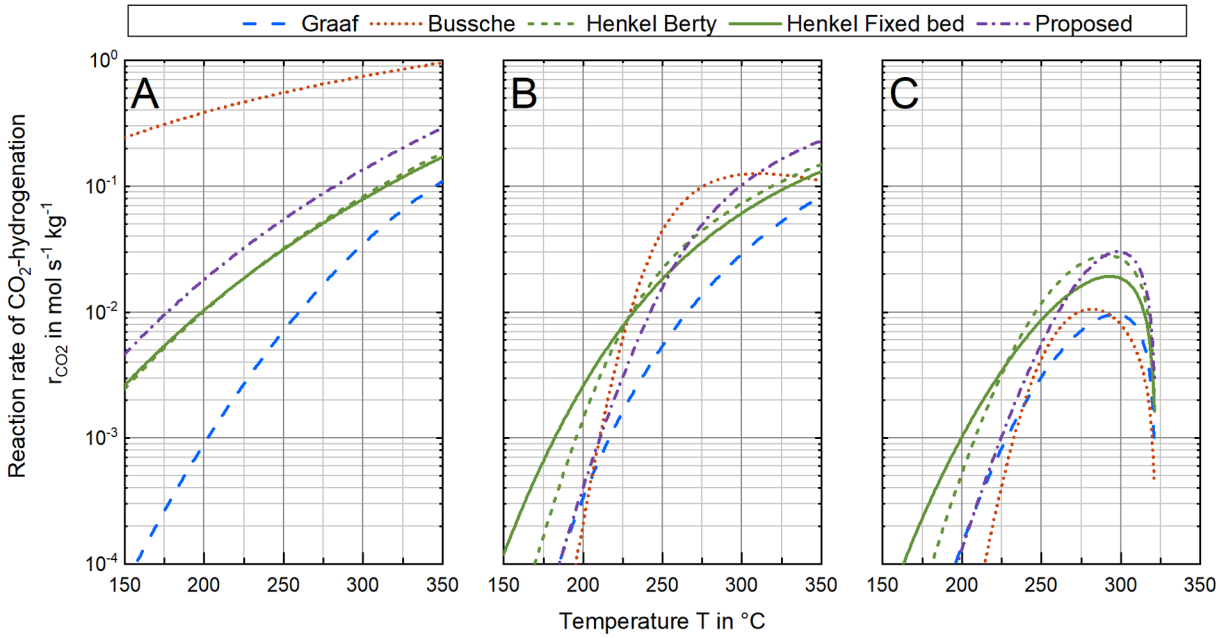

Fig. 4. Reaction rates of the kinetic models considered within this study at SN = 2.0, COR = 1.0, p = 50 bar without product (A), with approx. 0.5 mol-% methanol and 1.7 mol-% water (B), and 1.6 mol-% methanol and 4.5 mol-% water (C).

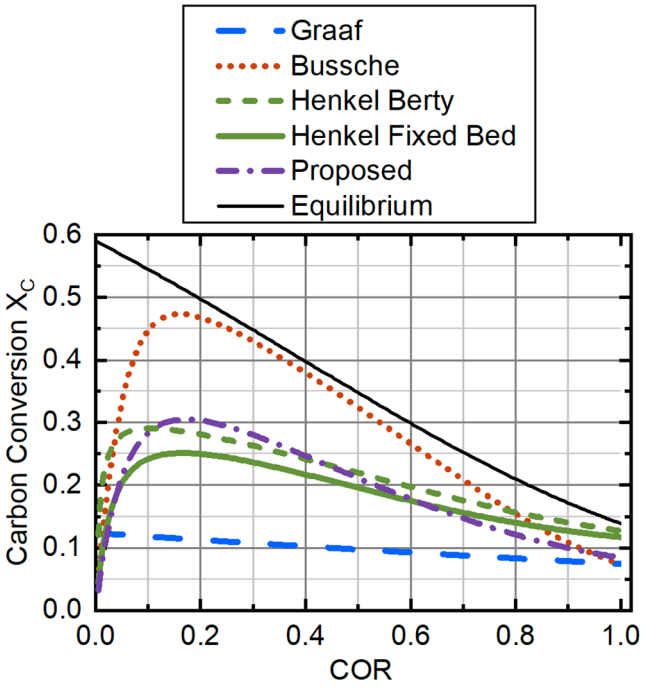

Fig. 5. Carbon conversion over COR at reactor inlet for the kinetic models by Graaf, Bussche, Henkel and the proposed model at a reaction pressure of 50 bar; SN adjusted towards 2.0; reaction temperature of 250 °C; GHSV of 20.000 h^{-1}; ideal isothermal reactor.

Reactor geometry data was applied as provided in Table 1.

The temperature profiles show that the kinetic model has a considerable effect on the hot spot formation in the reactor. Simulation with the kinetic model by Bussche leads to a hot spot temperature of 265 °C at an axial distance of 0.8 m while the proposed model reaches towards 268 °C at an axial position of 1.4 m. The axial difference between the models can be deduced from the high temperature rise at the reactor entry for approx. 5 K in the simulation using Bussche's model. This is interpreted as a result of the high initial reaction rate for CO_2 hydrogenation in absence of the products water and methanol (see Fig. 4). The temperature rise of the proposed model is in comparison to Bussche's model rather steady with a comparable gradient after the inlet zone.

The concentration profiles of the products are closely linked to the temperature profiles in the reactor. The model by Bussche shows a higher rate of methanol and water formation at the reactor entry in comparison to the proposed model. Nonetheless, both simulations approach equilibrium at cooling temperature at the reactor exit. rWGS producing water and CO reaches equilibrium faster than CO_2 hydrogenation. The slight increase in water concentration beyond the hot spot is mostly due to small variations in reactor temperature and consecutive equilibrium adaption of the reactants.

Based on the previously shown results, hot spot position and magnitude were used for an advanced analysis of the model behavior depending on COR, SN and synthesis pressure for the parameter range listed in Table 3. The data on position and temperature of the hot spot are presented in Fig. 7. As the parameter set which Henkel determined from the Berty reactor is based on a wider temperature range and higher pressures than the fixed bed, the latter was not considered within the sensitivity study. Pressures exceeding the valid range of the kinetic models were applied in the simulation as the extrapolation of the pressure range is commonly done in scientific publications performing reactor simulations [24,46,47,71,72].

Overall results from the sensitivity study show that the hot spot temperatures rise with increasing pressure and decreasing COR for all kinetic models. This behavior is in line with literature findings regarding the maximum methanol reaction rates and the increased exothermic heat at high CO contents in the reactor feed gas. The increase of reaction kinetics with increasing pressure is in agreement with Le Chatelier's principle. However, big differences in position and temperature of the hot spot were determined between the different kinetic models proving the necessity of an appropriate description of reaction kinetics for reactor design purposes. Among all considered kinetic models the lowest sensitivity of hot spot temperature and position towards COR is predicted by Graaf. In addition, this model delivers the lowest hot spot temperatures for the COR range between 0.25 and 0.75. The poor activity of Graaf's model was already documented within the scientific community [59] and could be due to the fact that the catalyst for Graaf's kinetic model was less active than those applied by other

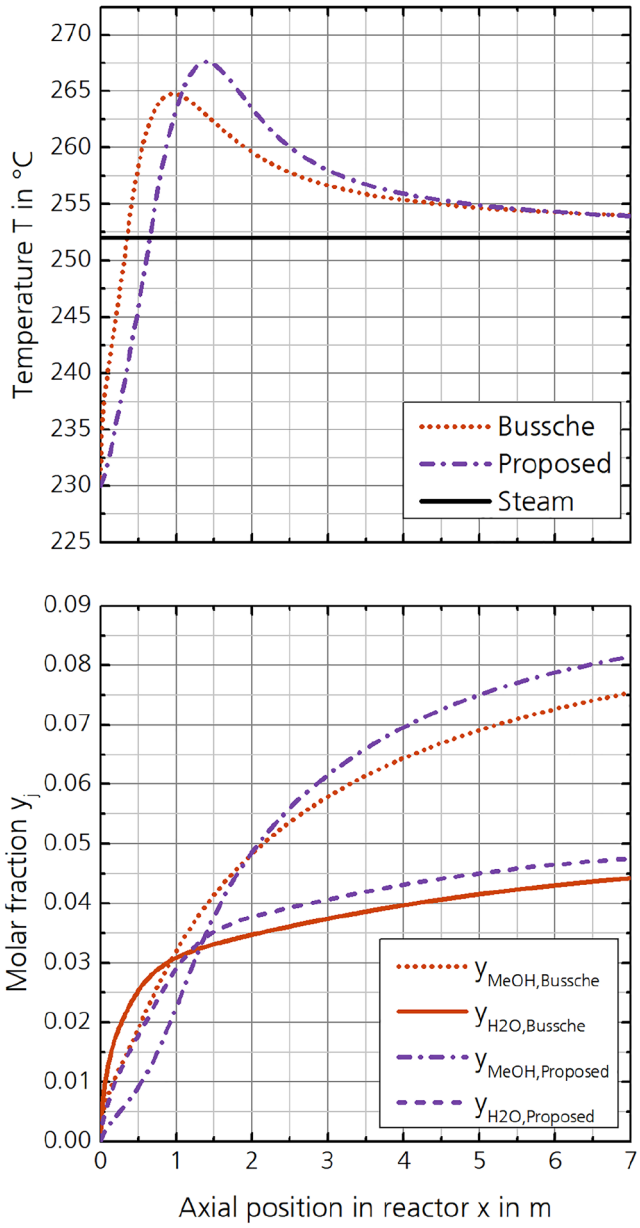

Fig. 6. Comparison of the 1D-temperature profiles (top) and product molar fraction profiles (bottom) obtained by a reactor simulation at COR = 0.75, SN = 2.0, GHSV = 10.000 h^{-1} at a pressure of 65 bar utilizing the kinetic model by Bussche and the proposed model; Design parameters applied according to Table 1.

researchers. Therefore, this model should be used with caution for the description of state-of-the-art methanol synthesis.

The kinetic model by Bussche provides a higher sensitivity towards changes in COR in comparison to Graaf. The highest temperatures are achieved at low SN-values for COR between 0.25 and 0.75. A strong decrease of the hot spot temperature can be denoted with increasing SN. This behavior is in contrast to the other kinetic models depicted in Fig. 7 as these show a slight increase of catalytic activity, i.e. higher hot spot temperatures and further upstream positions, with rising SN. An increase of the reaction rates with rising SN was also found by Chanchlani et al. who performed an experimental study on the influence of H_2 on the rate of methanol formation [64]. As the SN-range of the kinetic study was not documented within the publication by Bussche, the diverging behavior of this model could be explained by a missing variation of SN in their experimental campaign. Therefore, it can be stated, that the model by Bussche should be carefully applied with regard to variations in SN.

The hot spot temperatures and positions simulated with the model proposed by Henkel ranges between those predicted by Bussche and Graaf at COR between 0.25 and 0.75.

The kinetic model proposed within this study shows a comparable sensitivity towards COR as the model by Bussche, however, with the hot spot formed further downstream for COR ranging between 0.25 and 0.75 (also see Fig. 6). Synthesis pressure is predicted with a higher effect towards hot spot temperature as compared to Bussche. This is most likely due to the higher pressures applied in the experimental campaign for the proposed kinetic model (compare Fig. 1). The insufficient description of the reaction kinetics by Bussche at pressures exceeding 50 bar was already claimed by Mignard et al. proposing a pressure extension for this model [54,55]. However this extension was based on the measured data by Klier from 1982 and therefore most likely based on a different catalyst than the one applied within Bussche's study.

Due to the low reaction enthalpy of CO_2 hydrogenation coupled with the low equilibrium conversion, all kinetic models show low hot spot temperatures for the case of COR = 1.0. However, the maximum temperature rise slightly increases with rising SN. For the cases with COR = 1.0 the positions of the hot spots for the kinetic models by Bussche and the proposed kinetic model are almost similar, while Graaf and Henkel show the hot spot further upstream. The kinetic model by Henkel is most active for high CO_2 contents by means of hot spot temperature and position. This is most probably due to the fact that Henkel did not include measurements at high COR. Therefore, this model cannot account for the inhibiting effect of water at high COR appropriately [55,56,64].

Generally, the proposed kinetic model was proven to behave plausibly in comparison to the other kinetic models considered in this study. As this model covers the technical relevant pressure and COR range, it is likely that the trends shown by the sensitivity analysis are more realistic than those given by the other models.

4. Conclusion and outlook

For the application of kinetic models for methanol synthesis it is of significant importance that the relevant parameter range is considered, as the extrapolation of the catalytic activity is not necessarily valid as long as the mechanism of methanol synthesis is not understood completely. In this study, a kinetic model based on recent experimental data was presented. The model was validated against state-of-the-art models at technologically relevant operation conditions. Furthermore, a sensitivity analysis was performed within this work comparing the influence of the most important factors as pressure, COR and SN on the reaction rate and the hot spot characteristics. It can be concluded that the performance of the kinetic model proposed within this work is comparable to the model proposed by Bussche, however, with a more consistent behavior towards SN and validity for higher pressures. The sensitivity analysis demonstrated that Bussche's kinetic model shows an inverse sensitivity towards SN indicating an important inconsistency within the model. The kinetic model by Graaf was proven to be less active and sensitive towards COR than the other models considered in this study. Therefore, special caution should be taken applying this model for description of modern methanol synthesis reactors. As water has a strongly inhibiting effect on the kinetics of methanol synthesis, measurements with high CO_2 contents should be included into kinetic measurement campaigns, especially with regard to PtM applications. Exclusion of high CO_2 contents from the kinetic measurement could lead towards an overestimated model activity as shown with the kinetic model proposed by Henkel.

A better description of the diffusion and heat transfer models based on experimental validation, could further improve the quality of the reactor model presented within this study. One promising technology for the detection of hot spot position and magnitude is the fiber optic temperature measurement enabling a highly resolved axial temperature

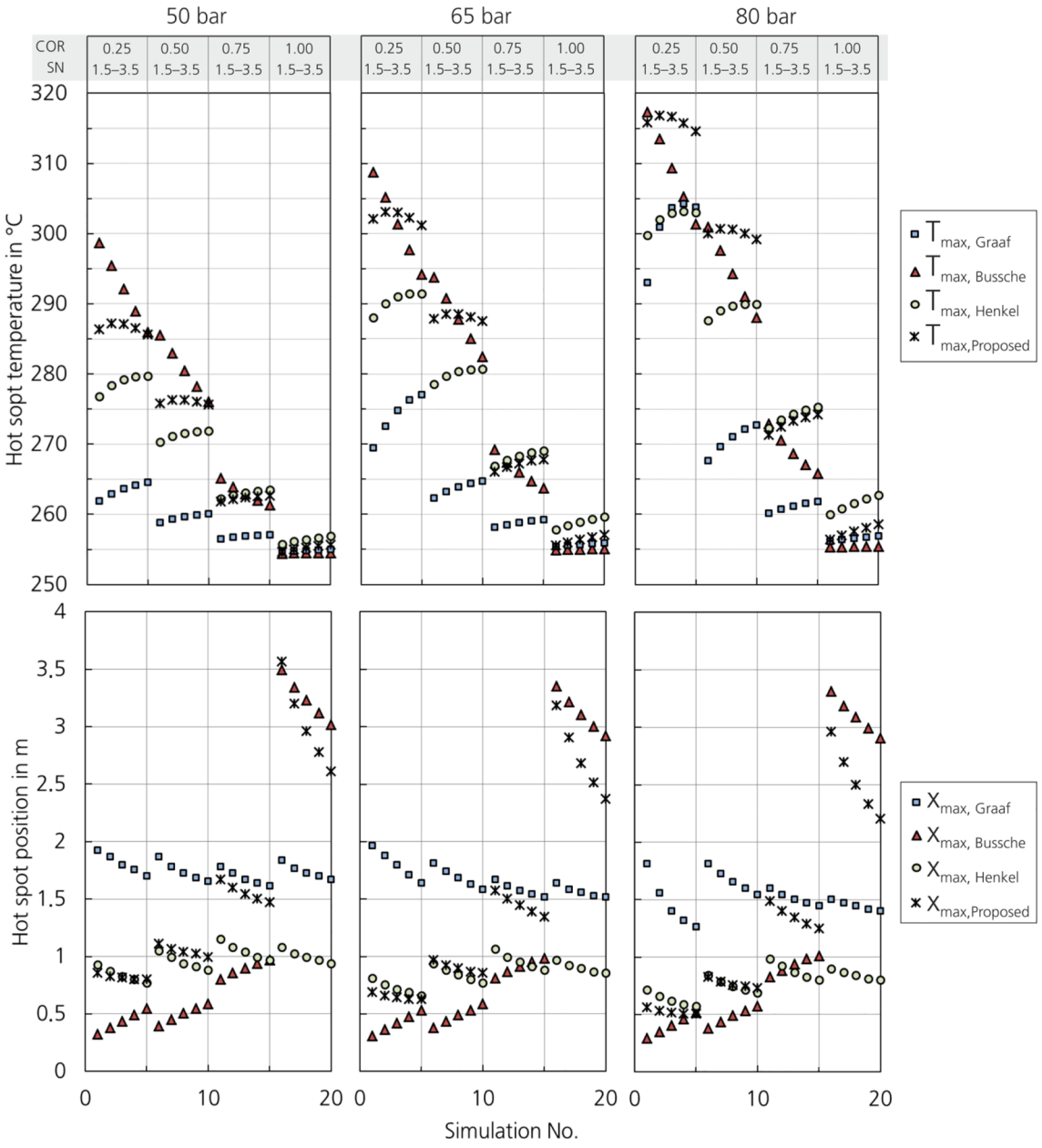

Fig. 7. Sensitivity study discussing the hot spot temperatures (top) and positions (bottom) obtained from the simulation of an industrial scale tubular reactor with the kinetic models by Graaf, Bussche and Henkel (Berty) as well as with the proposed kinetic model for the parameter range between $0.25 < COR < 1$, $1.5 < SN < 3.5$ at GHSV = 10.000 h^{-1} at the pressure levels of 50 bar, 65 bar and 80 bar; SN was varied in steps of 0.5; Design parameters applied according to Table 1.

analysis of the reactor [73]. An experimental setup including this feature is currently under development in our group.

Further experimental work will be necessary in order to evaluate the accuracy of the measured data published by Park et al. [20] and to gain a more robust validation base for the proposed kinetic model. Improved kinetic approaches could then be presented enabling a more accurate description of methanol synthesis. This would also enable the possibility of the description of unsteady state conditions as they might be faced by PtM processes in the future. To the best of our knowledge, the proposed kinetic model represents the most updated tool for the design of technical methanol synthesis reactors.

Declaration of Competing Interest

The authors declare that they have no known competing financial interests or personal relationships that could have appeared to influence the work reported in this paper.

Acknowledgements

This work was supported by the German Federal Ministry of Education and Research though the project Carbon2Chem® (03EK3039F). Deutsche Bundesstiftung Umwelt (DBU) is gratefully acknowledged for funding of the work of Florian Nestler (20017/517). Special thanks are dedicated to the team of Hydrogen Division at Fraunhofer Institute for Solar Energy Systems and the Division of Fuel Technology at Engler-Bunte-Institute at Karlsruhe Institute of Technology for their scientific support.

Appendix A

Mechanism on the catalyst surface proposed by Graaf [22]:
Adsorption:

$$CO + s1 \rightleftarrows CO^{(s1)} \tag{A.1}$$

$$CO_2 + s1 \rightleftarrows CO_2^{(s1)} \tag{A.2}$$

$$H_2 + 2s2 \rightleftarrows 2H^{(s2)} \tag{A.3}$$

$$H_2O + s2 \rightleftarrows H_2O^{(s2)} \tag{A.4}$$

Reaction path CO_2 hydrogenation:

$$CO_2^{(s1)} + H^{(s2)} \rightleftarrows HCO_2^{(s1)} + s2 \tag{A.5}$$

$$HCO_2^{(s1)} + H^{(s2)} \rightleftarrows H_2CO_2^{(s1)} + s2 \tag{A.6}$$

$$H_2CO_2^{(s1)} + H^{(s2)} \rightleftarrows H_3CO_2^{(s1)} + s2 \tag{A.7}$$

$$H_3CO_2^{(s1)} + H^{(s2)} \rightleftarrows H_2CO^{(s1)} + H_2O^{(s2)} \tag{A.8}$$

$$H_2CO^{(s1)} + H^{(s2)} \rightleftarrows H_3CO^{(s1)} + s2 \tag{A.9}$$

$$H_3CO^{(s1)} + H^{(s2)} \rightleftarrows H_3COH + s1 + s2 \tag{A.10}$$

Reaction path rWGS:

$$CO_2^{(s1)} + H^{(s2)} \rightleftarrows HCO_2^{(s1)} + s2 \tag{A.11}$$

$$HCO_2^{(s1)} + H^{(s2)} \rightleftarrows CO^{(s1)} + H_2O^{(s2)} \tag{A.12}$$

Reaction path CO hydrogenation:

$$CO^{(s1)} + H^{(s2)} \rightleftarrows HCO^{(s1)} + s2 \tag{A.13}$$

$$HCO^{(s1)} + H^{(s2)} \rightleftarrows H_2CO^{(s1)} + s2 \tag{A.14}$$

$$H_2CO^{(s1)} + H^{(s2)} \rightleftarrows H_3CO^{(s1)} + s2 \tag{A.15}$$

$$H_3CO^{(s1)} + H^{(s2)} \rightleftarrows H_3COH + s1 + s2 \tag{A.16}$$

Kinetic rate equations based on the mechanism described above:

$$r_{CO_2} = \frac{k_1 \cdot K_2 \cdot \left(f_{CO_2} \cdot f_{H_2}^{1.5} - \frac{f_{CH_3OH} \cdot f_{H_2O}}{f_{H_2}^{1.5} \cdot K_{eq,1}}\right)}{(1 + K_1 \cdot f_{CO} + K_2 \cdot f_{CO_2}) \cdot (f_{H_2}^{0.5} + K_3 \cdot f_{H_2O})} \tag{A.17}$$

$$r_{rWGS} = \frac{k_2 \cdot K_2 \cdot \left(f_{CO_2} \cdot f_{H_2} - \frac{f_{H_2O} \cdot f_{CO}}{K_{eq,2}}\right)}{(1 + K_1 \cdot f_{CO} + K_2 \cdot f_{CO_2}) \cdot (f_{H_2}^{0.5} + K_3 \cdot f_{H_2O})} \tag{A.18}$$

$$r_{CO} = \frac{k_3 \cdot K_1 \cdot \left(f_{CO_2} \cdot f_{H_2}^{1.5} - \frac{f_{CH_3OH} \cdot f_{H_2O}}{f_{H_2}^{1.5} \cdot K_{eq,1}}\right)}{(1 + K_1 \cdot f_{CO} + K_2 \cdot f_{CO_2}) \cdot (f_{H_2}^{0.5} + K_3 \cdot f_{H_2O})} \tag{A.19}$$

Table 6
Kinetic model parameters by Graaf [45].

	Unit	Kinetic parameters
k_1	$mol \cdot kg_{cat}^{-1} \cdot s^{-1} \cdot bar^{-1}$	$1.09 \cdot 10^{+5} \cdot \exp\frac{-87,500}{R \cdot T}$
k_2	$mol \cdot kg_{cat}^{-1} \cdot s^{-1} \cdot bar^{-0.5}$	$9.64 \cdot 10^{+11} \cdot \exp\frac{-152,900}{R \cdot T}$
k_3	$mol \cdot kg_{cat}^{-1} \cdot s^{-1} \cdot bar^{-1}$	$4.89 \cdot 10^{+7} \cdot \exp\frac{-113,000}{R \cdot T}$
K_1	bar^{-1}	$2.16 \cdot 10^{-5} \cdot \exp\frac{46,800}{R \cdot T}$
K_2	bar^{-1}	$7.05 \cdot 10^{-7} \cdot \exp\frac{61,700}{R \cdot T}$
K_3	$bar^{-0.5}$	$6.37 \cdot 10^{-9} \cdot \exp\frac{84,000}{R \cdot T}$

Appendix B

Mechanism on the catalyst surface proposed by Bussche et al. [18]:
Adsorption:

$$CO_2 + O^{(s)} + s \rightleftarrows CO_3^{(2s)} \quad \text{(B.1)}$$

$$CO_2 + s \rightleftarrows O^{(s)} + CO \quad \text{(B.2)}$$

$$H_2 + 2s \rightleftarrows 2H^{(s)} \quad \text{(B.3)}$$

$$H_2O + s \rightleftarrows H_2O^{(s)} \quad \text{(B.4)}$$

Reaction path CO_2 hydrogenation:

$$CO_3^{(2s)} + H^{(s)} \rightleftarrows HCO_3^{(2s)} + s \quad \text{(B.5)}$$

$$HCO_3^{(2s)} + s \rightleftarrows HCO_2^{(2s)} + O^{(s)} \quad \text{(B.6)}$$

$$HCO_2^{(2s)} + H^{(s)} \rightleftarrows H_2CO_2^{(2s)} + s \quad \text{(B.7)}$$

$$H_2CO_2^{(2s)} \rightleftarrows H_2CO^{(s)} + O^{(s)} \quad \text{(B.8)}$$

$$H_2CO^{(s)} + H^{(s)} \rightleftarrows H_3CO^{(s)} + s \quad \text{(B.9)}$$

$$H_3CO^{(s)} + H^{(s)} \rightleftarrows H_3COH + 2s \quad \text{(B.10)}$$

Reaction path rWGS:

$$O^{(s)} + H^{(s)} \rightleftharpoons OH^{(s)} + s \quad \text{(B.11)}$$

$$OH^{(s)} + H^{(s)} \rightleftharpoons H_2O^{(s)} + s \quad \text{(B.12)}$$

Kinetic rate equations based on the mechanism described above:

$$r_{CO_2} = \frac{k_1 \cdot f_{CO_2} \cdot f_{H_2} \cdot [1 - f_{H_2O} \cdot f_{CH3OH} / (f_{H_2}^3 \cdot f_{CO_2} \cdot K_{eq,1})]}{(1 + K_{1,B} \cdot (f_{H_2O}/f_{H_2}) + K_{2,B} \cdot f_{H_2}^{0,5} + K_{3,B} \cdot f_{H_2O})^3} \quad \text{(B.13)}$$

$$r_{rWGS} = \frac{k_2 \cdot f_{CO_2} \cdot [1 - f_{H_2O} \cdot f_{CO} / (f_{CO_2} \cdot f_{H_2} \cdot K_{eq,2})]}{(1 + K_{1,B} \cdot (f_{H_2O}/f_{H_2}) + K_{2,B} \cdot f_{H_2}^{0,5} + K_{3,B} \cdot f_{H_2O})} \quad \text{(B.14)}$$

Table 7
Kinetic model parameters by Bussche [18].

	Unit	Kinetic parameters
k_1	$mol \cdot kg_{cat}^{-1} \cdot s^{-1} \cdot Pa^{-2}$	$1.07 \cdot 10^{-10} \cdot \exp\frac{36,696}{R \cdot T}$
k_2	$mol \cdot kg_{cat}^{-1} \cdot s^{-1} \cdot Pa^{-1}$	$1.22 \cdot 10^{+5} \cdot \exp\frac{-94,765}{R \cdot T}$
$K_{1,B}$	–	3.45338
$K_{2,B}$	$Pa^{-0.5}$	$1.578 \cdot 10^{-3} \cdot \exp\frac{17,197}{R \cdot T}$
$K_{3,B}$	Pa^{-1}	$6.62 \cdot 10^{-16} \cdot \exp\frac{124,119}{R \cdot T}$

References

[1] Mark Bergren, Methanol to Energy – Challenges and Opportunities, Frankfurt, 2017.
[2] G. Bozzano, F. Manenti, Efficient methanol synthesis: perspectives, technologies and optimization strategies, Prog. Energy Combust. Sci. 56 (2016) 71–105, https://doi.org/10.1016/j.pecs.2016.06.001.
[3] J.T. Gallagher, J.M. Kidd GB000001159035A.
[4] J. Sehested, Industrial and scientific directions of methanol catalyst development, J. Catal. (2019), https://doi.org/10.1016/j.jcat.2019.02.002.
[5] S.G. Jadhav, P.D. Vaidya, B.M. Bhanage, J.B. Joshi, Catalytic carbon dioxide hydrogenation to methanol: a review of recent studies, Chem. Eng. Res. Des. 92 (2014) 2557–2567, https://doi.org/10.1016/j.cherd.2014.03.005.
[6] C. Li, X. Yuan, K. Fujimoto, Development of highly stable catalyst for methanol synthesis from carbon dioxide, Appl. Catal. A 469 (2014) 306–311, https://doi.org/10.1016/j.apcata.2013.10.010.
[7] J. Schumann, T. Lunkenbein, A. Tarasov, N. Thomas, R. Schlögl, M. Behrens, Synthesis and characterisation of a highly active Cu/ZnO: Al catalyst, ChemCatChem 6 (2014) 2889–2897, https://doi.org/10.1002/cctc.201402278.
[8] F. Nestler, M. Krüger, J. Full, M.J. Hadrich, R.J. White, A. Schaadt, Methanol synthesis – industrial challenges within a changing raw material landscape, Chem. Ing. Tech. 90 (2018) 1409–1418, https://doi.org/10.1002/cite.201800026.
[9] S. Dang, H. Yang, P. Gao, H. Wang, X. Li, W. Wei, Y. Sun, A review of research progress on heterogeneous catalysts for methanol synthesis from carbon dioxide hydrogenation, Catal. Today (2018). doi: 10.1016/j.cattod.2018.04.021.
[10] K.A. Ali, A.Z. Abdullah, A.R. Mohamed, Recent development in catalytic technologies for methanol synthesis from renewable sources: a critical review, Renew. Sustain. Energy Rev. 44 (2015) 508–518, https://doi.org/10.1016/j.rser.2015.01.010.
[11] G. Leonzio, E. Zondervan, P.U. Foscolo, Methanol production by CO2 hydrogenation: analysis and simulation of reactor performance, Int. J. Hydrogen Energy (2019), https://doi.org/10.1016/j.ijhydene.2019.02.056.
[12] R.O.d. Santos, L.d.S. Santos, D.M. Prata, Simulation and optimization of a methanol synthesis process from different biogas sources, J. Cleaner Prod. 186 (2018) 821–830, https://doi.org/10.1016/j.jclepro.2018.03.108.
[13] C. Hank, S. Gelpke, A. Schnabl, R.J. White, J. Full, N. Wiebe, T. Smolinka, A. Schaadt, H.-M. Henning, C. Hebling, Economics & carbon dioxide avoidance cost of methanol production based on renewable hydrogen and recycled carbon dioxide – power-to-methanol, Sustainable Energy Fuels (2018), https://doi.org/10.1039/

C8SE00032H.
[14] H.-W. Lim, M.-J. Park, S.-H. Kang, H.-J. Chae, J.W. Bae, K.-W. Jun, Modeling of the kinetics for methanol synthesis using Cu/ZnO/Al2O3/ZrO2 catalyst: influence of carbon dioxide during hydrogenation, Ind. Eng. Chem. Res. 48 (2009) 10448–10455, https://doi.org/10.1021/ie901081f.
[15] K. Kobl, S. Thomas, Y. Zimmermann, K. Parkhomenko, A.-C. Roger, Power-law kinetics of methanol synthesis from carbon dioxide and hydrogen on copper–zinc oxide catalysts with alumina or zirconia supports, Catal. Today 270 (2016) 31–42, https://doi.org/10.1016/j.cattod.2015.11.020.
[16] A. Coteron, A.N. Hayhurst, Kinetics of the synthesis of methanol from CO + H2 and CO + CO2 + H2 over copper-based amorphous catalysts, Chem. Eng. Sci. 49 (1994) 209–221, https://doi.org/10.1016/0009-2509(94)80039-1.
[17] X. An, Y. Zuo, Q. Zhang, J. Wang, Methanol synthesis from CO2 hydrogenation with a Cu/Zn/Al/Zr fibrous catalyst, Chin. J. Chem. Eng. 17 (2009) 88–94, https://doi.org/10.1016/S1004-9541(09)60038-0.
[18] K.M. Vanden Bussche, G.F. Froment, A steady-state kinetic model for methanol synthesis and the water gas shift reaction on a commercial Cu/ZnO/Al2O3 catalyst, J. Catal. 161 (1996) 1–10, https://doi.org/10.1006/jcat.1996.0156.
[19] T. Henkel, Modellierung von Reaktion und Stofftransport in geformten Katalysatoren am Beispiel der Methanolsynthese, PhD thesis Technical University of Munich, 2011.
[20] N. Park, M.-J. Park, Y.-J. Lee, K.-S. Ha, K.-W. Jun, Kinetic modeling of methanol synthesis over commercial catalysts based on three-site adsorption, Fuel Process. Technol. 125 (2014) 139–147, https://doi.org/10.1016/j.fuproc.2014.03.041.
[21] B. Vollbrecht, Zur Kinetik der Methanolsynthese an einem technischen Cu/ZnO/Al2O3-Katalysator. Dissertation, 2007.
[22] G.H. Graaf, E.J. Stamhuis, A.A.C.M. Beenackers, Kinetics of low-pressure methanol synthesis, Chem. Eng. Sci. 43 (1988) 3185–3195, https://doi.org/10.1016/0009-2509(88)85127-3.
[23] M.V. Twigg, M.S. Spencer, Deactivation of supported copper metal catalysts for hydrogenation reactions, Appl. Catal. A 212 (2001) 161–174, https://doi.org/10.1016/S0926-860X(00)00854-1.
[24] J.J. Meyer, P. Tan, A. Apfelbacher, R. Daschner, A. Hornung, Modeling of a methanol synthesis reactor for storage of renewable energy and conversion of CO_2 – comparison of two kinetic models, Chem. Eng. Technol. 39 (2016) 233–245, https://doi.org/10.1002/ceat.201500084.
[25] K. Aasberg-Petersen, I. Dybkjær, C.V. Ovesen, N.C. Schjødt, J. Sehested, S.G. Thomsen, Natural gas to synthesis gas – catalysts and catalytic processes, J. Nat. Gas Sci. Eng. 3 (2011) 423–459, https://doi.org/10.1016/j.jngse.2011.03.004.
[26] M. Bertau (Ed.), Methanol: The Basic Chemical and Energy Feedstock of the Future: Asinger's Vision Today, Springer, Berlin, Heidelberg, 2014.
[27] J. Skrzypek, M. Lachowska, M. Grzesik, J. Słoczyński, P. Nowak, Thermodynamics and kinetics of low pressure methanol synthesis, Chem. Eng. J. Biochem. Eng. J. 58 (1995) 101–108, https://doi.org/10.1016/0923-0467(94)02955-5.
[28] G.C. Chinchen, P.J. Denny, D.G. Parker, M.S. Spencer, D.A. Whan, Mechanism of methanol synthesis from CO2/CO/H2 mixtures over copper/zinc oxide/alumina catalysts: Use of 14C-labelled reactants, Appl. Catal. 30 (1987) 333–338, https://doi.org/10.1016/S0166-9834(00)84123-8.
[29] J.S. Lee, K.-Y. Lee, S.Y. Lee, Y.G. Kim, A comparative study of methanol synthesis from CO2/H2 and CO/H2 over a Cu/ZnO/Al2O3 catalyst, J. Catal. 144 (1993) 414–424, https://doi.org/10.1006/jcat.1993.1342.
[30] A.Y. Rozovskii, G.I. Lin, L.G. Liberov, E.V. Slivinskii, S.M. Loktev, Y.B. Kagan, A.N. Bashkirov, Mechanism of methanol synthesis from carbon-dioxide and hydrogen. 3. Determination of rates of individual stages using CO-14, Kinet. Catal. 18 (1977) 578–585.
[31] J. Schittkowski, H. Ruhland, D. Laudenschleger, K. Girod, K. Kähler, S. Kaluza, M. Muhler, R. Schlögl, Methanol synthesis from steel mill exhaust gases: challenges for the industrial Cu/ZnO/Al 2 O 3 catalyst, Chem. Ing. Tech. 115 (2018) 2, https://doi.org/10.1002/cite.201800017.
[32] A. Riaz, G. Zahedi, J.J. Klemeš, A review of cleaner production methods for the manufacture of methanol, J. Cleaner Prod. 57 (2013) 19–37, https://doi.org/10.1016/j.jclepro.2013.06.017.
[33] H.H. Kung, Deactivation of methanol synthesis catalysts – a review, Catal. Today 11 (1992) 443–453, https://doi.org/10.1016/0920-5861(92)80037-N.
[34] J.-P. Lange, Methanol synthesis: a short review of technology improvements, Catal. Today 64 (2001) 3–8, https://doi.org/10.1016/S0920-5861(00)00503-4.
[35] J. Ladebeck, Improve methanol synthesis, Hydrocarbon Processing;(United States) 72 (1993) 89–91.
[36] J. Wu, M. Saito, M. Takeuchi, T. Watanabe, The stability of Cu/ZnO-based catalysts in methanol synthesis from a CO2-rich feed and from a CO-rich feed, Appl. Catal. A 218 (2001) 235–240, https://doi.org/10.1016/S0926-860X(01)00650-0.
[37] M.B. Fichtl, D. Schlereth, N. Jacobsen, I. Kasatkin, J. Schumann, M. Behrens, R. Schlögl, O. Hinrichsen, Kinetics of deactivation on Cu/ZnO/Al2O3 methanol synthesis catalysts, Appl. Catal. A 502 (2015) 262–270, https://doi.org/10.1016/j.apcata.2015.06.014.
[38] F. Pontzen, W. Liebner, V. Gronemann, M. Rothaemel, B. Ahlers, CO2-based methanol and DME – Efficient technologies for industrial scale production, Catal. Today 171 (2011) 242–250, https://doi.org/10.1016/j.cattod.2011.04.049.
[39] K. Ushikoshi, K. Mori, T. Kubota, T. Watanabe, M. Saito, Methanol synthesis from CO2 and H2 in a bench-scale test plant, Appl. Organometal. Chem. 14 (2000) 819–825.
[40] G. Zahedi, A. Elkamel, A. Lohi, A. Jahanmiri, M.R. Rahimpour, Hybrid artificial neural network – First principle model formulation for the unsteady state simulation and analysis of a packed bed reactor for CO2 hydrogenation to methanol, Chem. Eng. J. 115 (2005) 113–120, https://doi.org/10.1016/j.cej.2005.08.018.
[41] H. Kordabadi, A. Jahanmiri, Optimization of methanol synthesis reactor using genetic algorithms, Chem. Eng. J. 108 (2005) 249–255, https://doi.org/10.1016/j.cej.2005.02.023.
[42] A. Elkamel, G. Reza Zahedi, C. Marton, A. Lohi, Optimal fixed bed reactor network configuration for the efficient recycling of CO2 into methanol, Energies 2 (2009) 180–189. doi: 10.3390/en20200180.
[43] F. Manenti, G. Bozzano, Optimal control of methanol synthesis fixed-bed reactor, Ind. Eng. Chem. Res. 52 (2013) 13079–13091, https://doi.org/10.1021/ie401511e.
[44] VDI-Wärmeatlas: Mit 320 Tabellen, 11th ed., Springer Vieweg, Berlin, 2013.
[45] G.H. Graaf, H. Scholtens, E.J. Stamhuis, A.A.C.M. Beenackers, Intra-particle diffusion limitations in low-pressure methanol synthesis, Chem. Eng. Sci. 45 (1990) 773–783, https://doi.org/10.1016/0009-2509(90)85001-T.
[46] F. Samimi, D. Karimipourfard, M.R. Rahimpour, Green methanol synthesis process from carbon dioxide via reverse water gas shift reaction in a membrane reactor, Chem. Eng. Res. Des. (2018), https://doi.org/10.1016/j.cherd.2018.10.001.
[47] A. Montebelli, C.G. Visconti, G. Groppi, E. Tronconi, S. Kohler, Optimization of compact multitubular fixed-bed reactors for the methanol synthesis loaded with highly conductive structured catalysts, Chem. Eng. J. 255 (2014) 257–265, https://doi.org/10.1016/j.cej.2014.06.050.
[48] M. Khanipour, A. Mirvakili, A. Bakhtyari, M. Farniaei, M.R. Rahimpour, A membrane-assisted hydrogen and carbon oxides separation from flare gas and recovery to a commercial methanol reactor, Int. J. Hydrogen Energy (2019), https://doi.org/10.1016/j.ijhydene.2019.04.149.
[49] S.S. Iyer, T. Renganathan, S. Pushpavanam, M. Vasudeva Kumar, N. Kaisare, Generalized thermodynamic analysis of methanol synthesis: effect of feed composition, J. CO2 Util. 10 (2015) 95–104, https://doi.org/10.1016/j.jcou.2015.01.006.
[50] É.S. Van-Dal, C. Bouallou, Design and simulation of a methanol production plant from CO2 hydrogenation, J. Cleaner Prod. 57 (2013) 38–45, https://doi.org/10.1016/j.jclepro.2013.06.008.
[51] G.H. Graaf, J.G.M. Winkelman, Chemical equilibria in methanol synthesis including the water-gas shift reaction: a critical reassessment, Ind. Eng. Chem. Res. 55 (2016) 5854–5864, https://doi.org/10.1021/acs.iecr.6b00815.
[52] G. Soave, Equilibrium constants from a modified Redlich-Kwong equation of state, Chem. Eng. Sci. 27 (1972) 1197–1203, https://doi.org/10.1016/0009-2509(72)80096-4.
[53] K.L. Ng, D. Chadwick, B.A. Toseland, Kinetics and modelling of dimethyl ether synthesis from synthesis gas, Chem. Eng. Sci. 54 (1999) 3587–3592, https://doi.org/10.1016/S0009-2509(98)00514-4.
[54] D. Mignard, C. Pritchard, On the use of electrolytic hydrogen from variable renewable energies for the enhanced conversion of biomass to fuels, Chem. Eng. Res. Des. 86 (2008) 473–487, https://doi.org/10.1016/j.cherd.2007.12.008.
[55] K. Klier, Catalytic synthesis of methanol from CO/H2IV. The effects of carbon dioxide, J. Catalysis 74 (1982) 343–360, https://doi.org/10.1016/0021-9517(82)90040-9.
[56] P. Nowak, M. Lachowska, J. Skrzypek, Influence of water vapour on methanol synthesis over CuO-ZnO-Al2O3 catalyst, Chem. Eng. Sci. 46 (1991) 3324–3325.
[57] J.A. Nelder, R. Mead, A simplex method for function minimization, Comput. J. 7 (1965) 308–313, https://doi.org/10.1093/comjnl/7.4.308.
[58] L. Chen, Q. Jiang, Z. Song, D. Posarac, Optimization of methanol yield from a Lurgi reactor, Chem. Eng. Technol. 34 (2011) 817–822, https://doi.org/10.1002/ceat.201000282.
[59] A. Montebelli, C.G. Visconti, G. Groppi, E. Tronconi, C. Ferreira, S. Kohler, Enabling small-scale methanol synthesis reactors through the adoption of highly conductive structured catalysts, Catal. Today 215 (2013) 176–185, https://doi.org/10.1016/j.cattod.2013.02.020.
[60] F. Manenti, S. Cieri, M. Restelli, G. Bozzano, Dynamic modeling of the methanol synthesis fixed-bed reactor, Comput. Chem. Eng. 48 (2013) 325–334, https://doi.org/10.1016/j.compchemeng.2012.09.013.
[61] F. Manenti, S. Cieri, M. Restelli, Considerations on the steady-state modeling of methanol synthesis fixed-bed reactor, Chem. Eng. Sci. 66 (2011) 152–162, https://doi.org/10.1016/j.ces.2010.09.036.
[62] M. Peter, M.B. Fichtl, H. Ruhland, S. Kaluza, M. Muhler, O. Hinrichsen, Detailed kinetic modeling of methanol synthesis over a ternary copper catalyst, Chem. Eng. J. 203 (2012) 480–491, https://doi.org/10.1016/j.cej.2012.06.066.
[63] G. Liu, The rate of methanol production on a copper-zinc oxide catalyst: The dependence on the feed composition, J. Catal. 90 (1984) 139–146, https://doi.org/10.1016/0021-9517(84)90094-0.
[64] K.G. Chanchlani, Methanol synthesis from H2, CO, and C02 over Cu/ZnO catalysts, J. Catal. 136 (1992) 59–75, https://doi.org/10.1016/0021-9517(92)90106-R.
[65] G.C. Chinchen, P.J. Denny, J.R. Jennings, M.S. Spencer, K.C. Waugh, Synthesis of Methanol, Applied Catalysis 36 (1988) 1–65, https://doi.org/10.1016/S0166-9834(00)80103-7.
[66] M. Takagawa, Study on reaction rates for methanol synthesis from carbon monoxide, carbon dioxide, and hydrogen, J. Catal. 107 (1987) 161–172, https://doi.org/10.1016/0021-9517(87)90281-8.
[67] Z.-X. Ren, J. Wang, J.-J. Jia, D.-S. Lu, Effect of carbon dioxide on methanol synthesis over different catalysts, Appl. Catal. 49 (1989) 83–90, https://doi.org/10.1016/S0166-9834(00)81424-4.
[68] M.A. McNeil, C.J. Schack, R.G. Rinker, Methanol synthesis from hydrogen, carbon monoxide and carbon dioxide over a CuO/ZnO/Al2O3 catalyst, Appl. Catal. 50

(1989) 265–285, https://doi.org/10.1016/S0166-9834(00)80841-6.
[69] B. Denise, R.P.A. Sneeden, C. Hamon, Hydrocondensation of carbon dioxide: IV, J. Mol. Catal. 17 (1982) 359–366, https://doi.org/10.1016/0304-5102(82)85047-5.
[70] C. Kuechen, U. Hoffmann, Investigation of simultaneous reaction of carbon monoxide and carbon dioxide with hydrogen on a commercial copper/zinc oxide catalyst, Chem. Eng. Sci. 48 (1993) 3767–3776, https://doi.org/10.1016/0009-2509(93)80219-G.
[71] R. de María, I. Díaz, M. Rodríguez, A. Sáiz, Industrial methanol from syngas: kinetic study and process simulation, Int. J. Chem. Reactor Eng. 11 (2013), https://doi.org/10.1515/ijcre-2013-0061.
[72] J.G. van Bennekom, J.G.M. Winkelman, R.H. Venderbosch, S.D.G.B. Nieland, H.J. Heeres, Modeling and experimental studies on phase and chemical equilibria in high-pressure methanol synthesis, Ind. Eng. Chem. Res. 51 (2012) 12233–12243, https://doi.org/10.1021/ie3017362.
[73] J. Schwarz, D. Samiec (Eds.), B3.4 – Fiber-Optic Measurement of Temperature Profiles. AMA Service GmbH, Von-Münchhausen-Str. 49, 31515 Wunstorf, Germany, 2017.